An Approach for Load Shedding in Islanded Microgrids

Wesley Peres*. Francisco C. R. Coelho*. Raphael P. B. Poubel**. Junior N. N. Costa*

*Departamento de Engenharia Elétrica, Universidade Federal de São João del Rei – UFSJ, São João del-Rei, Minas Gerais, Brasil (e-mail: wesley.peres@ufsj.edu.br; franciscocoelho@ufsj.edu.br; juniornatanncosta@gmail.com)

** Departamento de Engenharia Elétrica, Centro Federal de Educação Tecnológica de Minas Gerais – CEFET-MG, Belo Horizonte, Brasil (e-mail: poubel@cefetmg.br)

Abstract: This paper proposes an Optimal Power Flow for defining the minimum load to be shed to maintain the steady-state frequency between allowable limits in islanded microgrids. The droop coefficients and setpoints (no-load voltage and frequency of each Distributed Generator) are optimized considering the limits of microgrid frequency, nodal voltages, and power generation (apparent and reactive powers). The approach is applied to a microgrid of 33 nodes, considering a 24 hours time-horizon. The found results point to the methodology effectiveness.

Keywords: Microgrid, Islanded Operation, Load Shedding, Optimal Power Flow, Steady-State Frequency Regulation

1. INTRODUCTION

Microgrids (MG) has been subject of several works in the literature in the last years. The MG can be defined as a low-voltage system composed of controllable (dispatchable, like diesel generators) and uncontrollable (non-dispatchable, like wind turbines and photovoltaic systems) Distributed Generators (DG), storage systems (such as batteries), controllers, loads, and communication systems. In this context, MG has become an essential part of Distribution Systems, comprising a trade-off between reliability, quality and sustainability in energy supply (Foroutan et al., 2016).

An MG can be operated in two modes: connected to the upstream grid or in an islanded (isolated) mode. When connected with the main grid, distributed generators are operated as generation sources in PQ or PV modes, injecting power into the system, being the upstream grid responsible for maintaining the power balance and MG frequency in the face of load variations (Lopes et al., 2006). In this case, conventional computational tools can be used for planning the MG operation, like Power Flow (PF) and Optimal Power Flow (OPF) based on the use of swing bus (the main grid acts as the swing node, capable of supply losses and demand variations). For isolated mode, special attention must be paid due to the usual DG low-inertia characteristic. Since there is no distributed generator with capacity (MVA) to perform the power balance, load variations and losses must be shared among all units based on the Droop Method (Lopes et al., 2006). In this case, the MG frequency can not be maintained at the nominal value and it varies according to the load variation. DG are connected to MG through power electronics converters, being the voltage and frequency control forcibly similar to those performed for synchronous generators at the main grid (La Gatta et al., 2019).

Since there is no DG unit to act as a swing bus, computational tools must take this peculiarity into account. In (La Gatta et al., 2019), a Newton-Raphson-based approach is proposed to solve the governor power flow in polar coordinates. In (Alves et al., 2019), the methodology presented in (La Gatta et al., 2019) has been solved by using the current injection equations. In addition, it is essential to assess the static voltage stability, as it has recently been addressed in (de Nadai Nascimento et al., 2021).

In planning studies, Optimal Power Flow (OPF) approaches play an important role, and many methods have been proposed to solve it since the seventies (Dommel & Tinney, 1968; Granville, 1994). Again, the absence of the slack node makes conventional OPF approaches inappropriate for islanded MG. Therefore, in the last decade, the inclusion of frequency and voltage droop characteristics of distributed generators into the OPF has been investigated in the literature (Foroutan et al., 2016; Hemmatpour et al., 2016; La Gatta et al., 2019; Manna et al., 2018).

In (Hemmatpour et al., 2016), a Multiobjective Harmony Search Algorithm is proposed to maximize the MG loadability and to minimize the system losses through the islanded reconfiguration. The approach is validated by using the 33 and 69 nodes microgrids. In (Manna et al., 2018), an optimization technique employing the Artificial Bee Colony Algorithm is proposed for loss minimization. The droop coefficients of multiple generators are optimized for a 38-bus microgrid. In (Foroutan et al., 2016), the Genetic Algorithm and the Harmony Search Algorithm are hybridized to solve a multiobjective problem that minimizes fuel consumption costs and maximizes a voltage stability index. The studies are performed employing the 33 and 69 nodes islanded microgrid. Microgrids can operate in the islanded condition all the time or in a pre-specified period due to large-scale events that disconnect parts of the system (La Gatta et al., 2019). In the

latter case, if it is known the period that the system will be isolated, actions can be planned to minimize the negative impacts to customers and the grid. In general, the DG units (controllable or uncontrollable) have not enough capacity to ensure the operation at the nominal frequency and actions like load shedding must be carried out to keep the MG frequency between specified limits (Bakar et al., 2017).

In (La Gatta et al., 2019), an OPF is proposed to define the minimum amount of load to be shed to maintain the MG frequency between specified limits. The frequency and voltage droop of DG units are considered. However, droop coefficients and setpoints (like no-load voltage and frequency of each DG) are considered to be known. The methodology is validated for a 61-bus radial system.

This paper proposes an Optimal Power Flow for defining the minimum load to be shed to maintain the steady-state frequency between allowable limits. The generators' droop coefficients and setpoints are optimized considering the MG frequency, nodal voltages, and power generation limits. For validation, the approach is applied to a microgrid of 33 nodes (Foroutan et al., 2016) considering a time-horizon 24 hours.

2. PROPOSED APPROACH

2.1 Droop Characteristic

Figure 1 depicts the $P - f$ and $Q - V$ droop characteristics of a generator. The active and reactive power generations (P_{gk} and Q_{gk}) can be calculated through the mathematical expressions presented in equations (1)-(2).
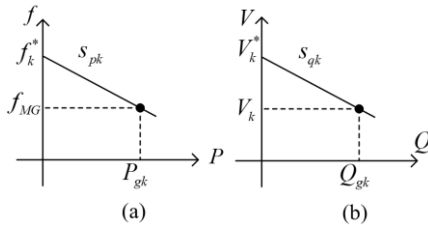

Figure 1. Droop characteristics: (a) $P - f$ droop, (b) $Q - V$ droop

$$P_{gk} = \frac{1}{s_{pk}} . (f_k^* - f_{MG}) \qquad (1)$$

$$Q_{gk} = \frac{1}{s_{qk}} . (V_k^* - V_k) \qquad (2)$$

where f_{MG} is the frequency of the MG; V_k is the terminal voltage of the kth generator; f_k^* and V_k^* are the reference of f_{MG} and V_k at no load, respectively; s_{pk} and s_{qk} are the droop coefficients, respectively.

2.2 Proposed OPF Formulation

Equation (3) brings the general formulation of an OPF, being $\underline{x}$ the vector of control and state variables, $F(\underline{x})$ is the objective function, $\underline{h}(\underline{x})$ and $\underline{g}(\underline{x})$ are the sets of equality and inequality constraints, $\underline{lb}$ and $\underline{ub}$ are the lower and upper bounds of variables.

$$
\begin{aligned}
minimize \quad & F(\underline{x}) \\
& \underline{h}(\underline{x}) = 0 \\
subject\ to \quad & \underline{g}(\underline{x}) \leq 0 \\
& \underline{lb} \leq \underline{x} \leq \underline{ub}
\end{aligned} \qquad (3)
$$

The objective function $F(\underline{x})$ in equation (3) is detailed in equation (4), which is the sum of total load to be shed: C_k is the cost of load to be shed at bus k (in this paper is considered to be 1 for all loads); α_k is the percentage of load to be shed at bus k; P_{dk} is the active power load at bus k; Ω_B is the set of nodes of the system.

$$min \quad F = \sum_{k \in \Omega_B} C_k . \alpha_k . P_{dk} \qquad (4)$$

The set of equality constraints in equation (3) is composed of equations (5)-(10). The active and reactive power balance at each node k are given in equations (5)-(6): Q_{dk} is the reactive power load at bus k; P_k and Q_k are the active and reactive power injections, calculated according to (Gómez-Expósito et al., 2017). It is important to emphasize that, in this paper, the voltage and frequency dependence of load is not considered (Kundur, 1994). The $P - f$ and $Q - V$ droop characteristics are given in equations (7)-(8), being Ω_G the set of generators. Equation (9) provides an angular reference for the system (any node k can be set as the reference one). Finally, equation (10) expresses the apparent power S_{gk} as a function of active and reactive power generations.

$$P_{gk} - (1 - \alpha_k) . P_{dk} - P_k = 0 \qquad (k \in \Omega_B) \qquad (5)$$

$$Q_{gk} - (1 - \alpha_k) . Q_{dk} - Q_k = 0 \qquad (k \in \Omega_B) \qquad (6)$$

$$P_{gk} - \frac{1}{s_{pk}} . (f_k^* - f_{MG}) = 0 \qquad (k \in \Omega_G) \qquad (7)$$

$$Q_{gk} - \frac{1}{s_{qk}} . (V_k^* - V_k) = 0 \qquad (k \in \Omega_G) \qquad (8)$$

$$\theta_k^{ref} = 0 \qquad (9)$$

$$S_{gk} - \sqrt{(P_{gk})^2 + (Q_{gk})^2} = 0 \qquad (k \in \Omega_G) \qquad (10)$$

The set of inequality constraints $\underline{g}(\underline{x})$ in (3) is composed of equations (11) and (12), where S_{gk}^{max} is the maximum generation apparent power of generator k.

$$S_{gk} \leq S_{gk}^{max} \quad (k \in \Omega_G) \qquad (11)$$

$$P_{gk} \geq 0 \qquad (k \in \Omega_G) \qquad (12)$$

Finally, the lower and upper bounds in equation (3) are detailed in (13)-(20), for the: reactive power generations Q_{gk}, percentage of load to be shed at bus k α_k, frequency of the microgrid f_{MG}, nodal voltages V_k (including the terminal voltage of generators), reference frequencies at no-load f_k^*, reference voltages at no-load V_k^*, $P - f$ droop coefficients s_{pk} and $Q - V$ droop coefficients s_{qk}.

$$Q_{gk}^{min} \leq Q_{gk} \leq Q_{gk}^{max} \qquad (k \in \Omega_G) \qquad (13)$$

$$0 \leq \alpha_k \leq 1 \qquad (k \in \Omega_B) \qquad (14)$$

$$f_{min} \leq f_{MG} \leq f_{max} \qquad (15)$$

$$V_{min} \leq V_k \leq V_{max} \qquad (k \in \Omega_B) \qquad (16)$$

$$f_k^{*\,min} \leq f_k^* \leq f_k^{*\,max} \qquad (k \in \Omega_G) \qquad (17)$$

$$V_k^{*\,min} \leq V_k^* \leq V_k^{*\,max} \qquad (k \in \Omega_G) \qquad (18)$$

$$s_{pk}^{min} \leq s_{pk} \leq s_{pk}^{max} \qquad (k \in \Omega_G) \qquad (19)$$

$$s_{qk}^{min} \leq s_{qk} \leq s_{qk}^{max} \qquad (k \in \Omega_G) \qquad (20)$$

It is important to emphasize that the inclusion of the constraints (17)-(20) in an OPF to define the minimum amount of load to be shed to maintain the steady-state frequency between allowable limits is a little contribution of this paper, in comparison to the approach recently proposed in (La Gatta et al., 2019).

In (Jithendranath et al., 2021), the droop coefficients are also considered as optimization variables in a multi-objective approach (solved the NSGA-II and MPSO) that minimizes the generation costs, pollution emission and voltage deviations.

The proposed methodology was implemented using the solver *fmincon* of the optimization toolbox of the MatLab™ platform (version 2010a) (MathWorks, 2020). This solver is based on the Interior Point Method (Granville, 1994).

2.3 Time-Horizon

This paper considers that the islanded condition results from a perturbation, and the microgrid will be connected to the upstream grid after a known time-horizon (here, 24 hours). In this case, the base case previously presented in (Baran & Wu, 1989; Foroutan et al., 2016; Hemmatpour et al., 2016) is subjected to a load curve, and the proposed approach is applied 24 times to define the total amount of load to be shed in each hour. It is relevant that the proposed approach can be modified to consider energy storage systems (causing a coupling between load stages) (Pulendran & Tate, 2017). This is a feature to be investigated in the future.

3. RESULTS

3.1 System Description

The preliminary results obtained by using the proposed approach are presented in this section for a 33-bus-islanded microgrid. The original data at the base case (for power loads and distribution lines) are available in (Baran & Wu, 1989). An islanded-microgrid arises from the disconnection between nodes 33 (substation) and 1, as shown in Figure 2 (node 1 is taken as the reference one). As considered in (Foroutan et al., 2016), three controllable (dispatchable, like diesel generators) DG are available at nodes 21, 24 and 25. The base power and

the base voltage are 1 MVA and 12.66 kV, respectively. Table 1 brings the data of DG units. The bounds of frequencies, voltages and droop coefficients are presented in Table 2. These values were defined accordingly to the literature (Foroutan et al., 2016; Gupta et al., 2021).
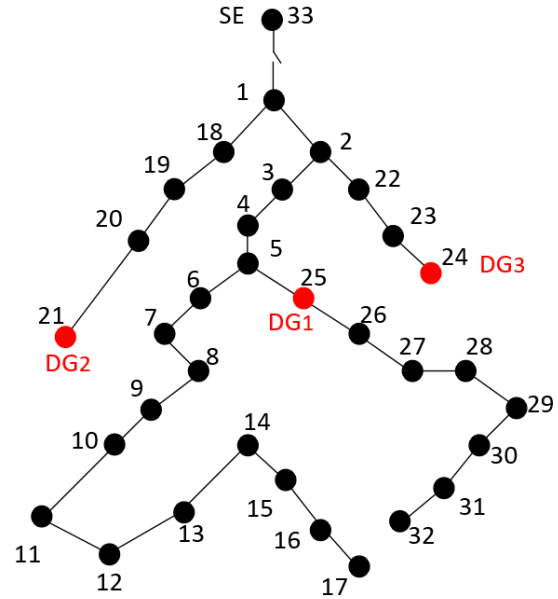

Figure 2. 33-bus-islanded microgrid system

TABLE 1. DATA OF DG UNITS

DG	Node	S_g^{max} (MVA)	Q_g^{min} (Mvar)	Q_g^{max} (Mvar)
1	25	3.0	-1.2	1.2
2	21	1.0	-0.6	0.6
3	24	1.5	-0.9	0.9

TABLE 2. BOUNDS

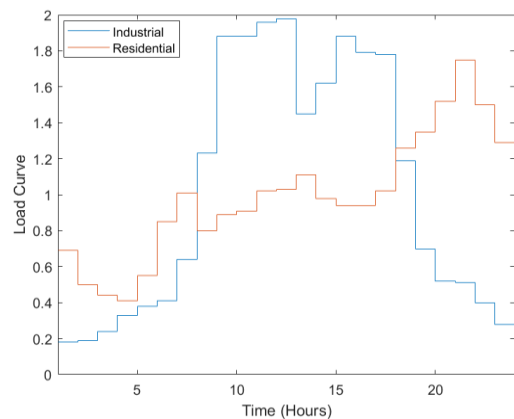| Variable	Lower	Upper
f_{MG} (Hz)	59.8	60.3
V_k (pu)	0.9	1.1
f_k^* (Hz)	59.8	60.3
V_k^* (pu)	0.9	1.1
s_{pk} (pu)	1.0e-5	1.0e-1
s_{qk} (pu)	1.0e-5	1.0e-2

Figure 3. Load curve

A load curve is used to evaluate the proposed approach considering a time horizon of 24 hours, as depicted in Figure 3 (multiplicative factors applied to the base case). Nodes 23, 24, 29 and 30 are supposed to be industrial, and the remaining, residential ones.

3.2 Results

Figure 4 depicts the resulting steady-state frequency of the MG at each hour, when applying the proposed methodology. It is possible to see that the minimum frequency limit criteria (59.80 Hz) has been met.

In this case, the frequency ranges from 59.87 Hz to 59.88 Hz after the load shedding. It is in accordance with Figures 9 e 10: the reference frequency of each generator is around 60.1 Hz (Figure 9), while the $P - f$ droop coefficients (s_{pk}) (Figure 10) are higher than $Q - V$ droop coefficients (s_{qk}) (Figure 13). Therefore, there is a higher frequency droop.

From Figures 8 and 15 to 17, it can be seen that the microgrid has the required power capacity to supply the loads. Otherwise, the power generation would achieve its limits (Table 1): in this case, the load shedding would occur because of the lack of generation support, and the frequency could be higher than 59.8 Hz (the lower limit). Since the system has enough power generation capacity, a globally optimal solution would provide $f_{MG} = 59.80\ Hz$ (and it has not occurred), indicating that the obtained solution is possible a local one. It shows that the problem under analysis has a multimodal nature.

As expected, analytical optimization methods (as the one employed by the solver *fmincon*) can fail in providing the best solution (global one), as a result, for instance, of their high sensitivity to initial conditions. This fact does not impair the proposed approach's application since other solvers can be employed (to search for the global best solution) (La Gatta et al., 2019). Besides, a more detailed investigation regarding the initial conditions used can enhance the result's quality. Finally, metaheuristic-based optimization methods are very attractive to solve these problems and will be investigated in the future by the authors (Peres et al., 2015).
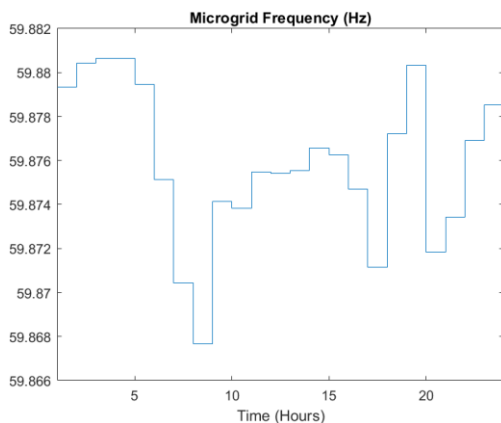

Figure 4. Microgrid frequency

The total amount of load shed is brought in Figures 5 to 7 and 14. A significant decrease in total load is enforced. Figures 7 and 8 show that the apparent power generation capacity of the system (5.5 pu) is not reached after the load shedding: figures 15 to 17 detail the generation power of each unit, showing that

limits were not reached. As a result of the droop characteristic, the load must be shed to meet the frequency criteria, even if the system has generation capacity.

Finally, Figures 9 to 13 bring the reference (setpoint) frequencies, reference voltages, and the droop coefficients adjusted for each hour. The suitable tuning of these parameters provides flexibility to the microgrid operation: since the load changes during the day, it is important to exploit the possibility of setting different values for each hour. For example, by properly choosing s_{pk} and f_k^* of a given generator, the same active power can be dispatched under different frequencies.

For the sake of completeness, the average computational burden associated with each time horizon was around 3.6 seconds in an Intel Core i7 1.80 GHz computer with 8 GB of RAM and Windows 10 64-bit operating system.
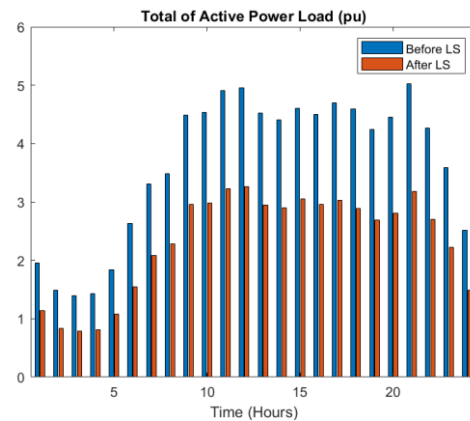

Figure 5. Active power load before and after the load shedding (LS)
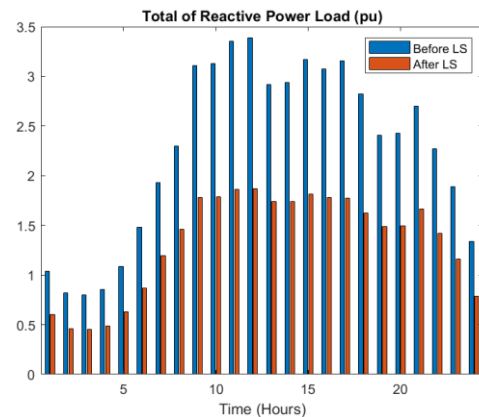

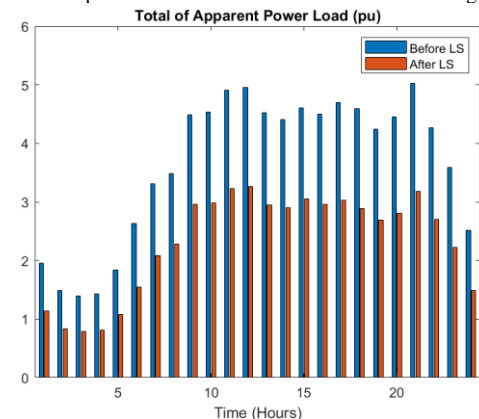Figure 6. Reactive power load before and after the load shedding (LS)

Figure 7. Apparent power load before and after the load shedding (LS)
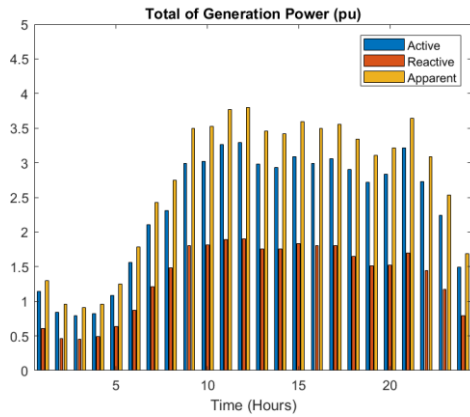
Figure 8. Total of generation after the load shedding
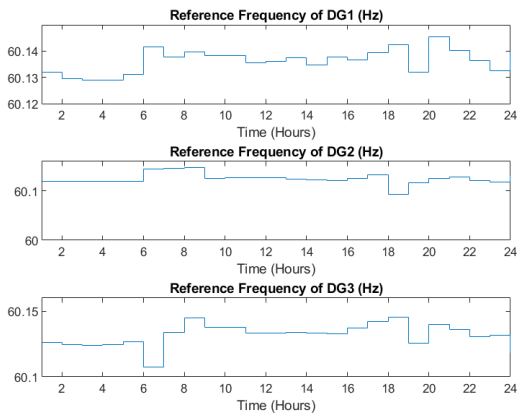

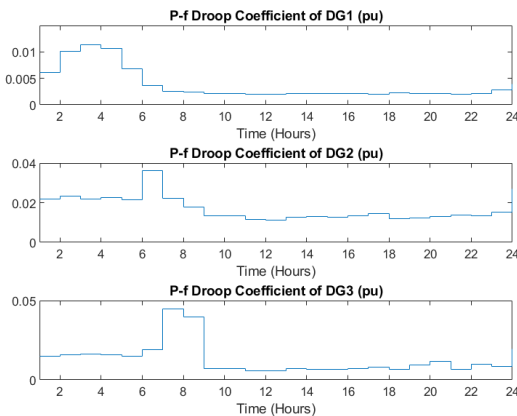Figure 9. Reference frequency of DG units

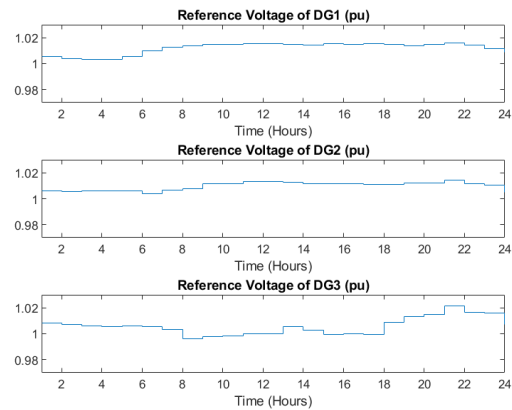Figure 10. $P - f$ droop coefficient of DG units

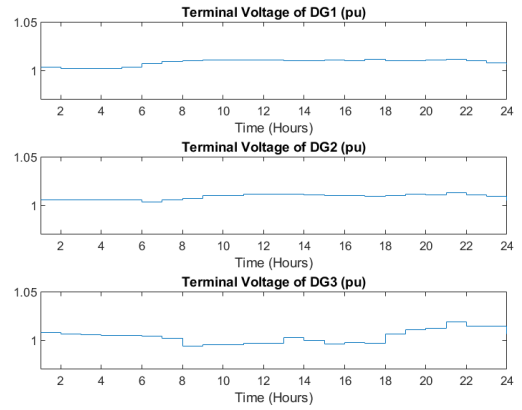

Figure 11. Reference voltage of DG units

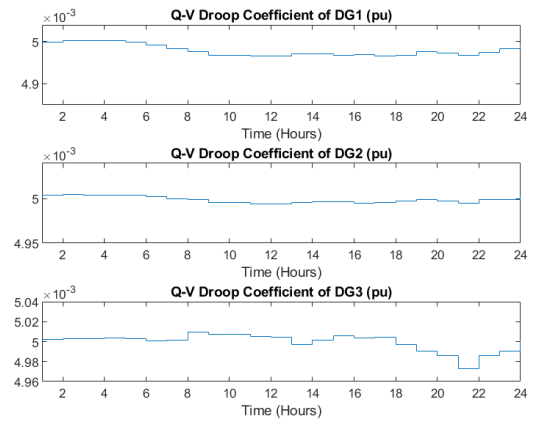Figure 12. Terminal voltage of DG units

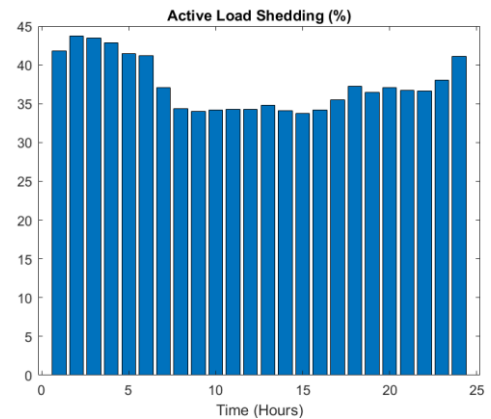Figure 13. $Q - V$ droop coefficient of DG units

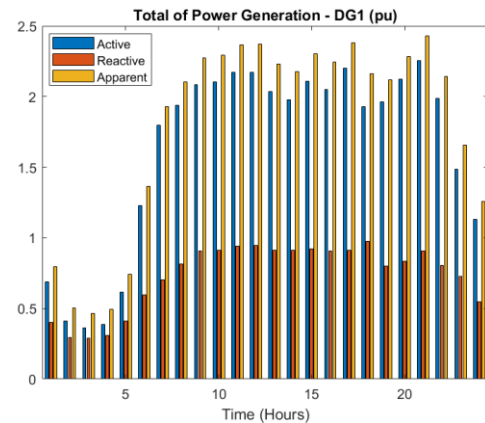

Figure 14. Loading shedding percentage
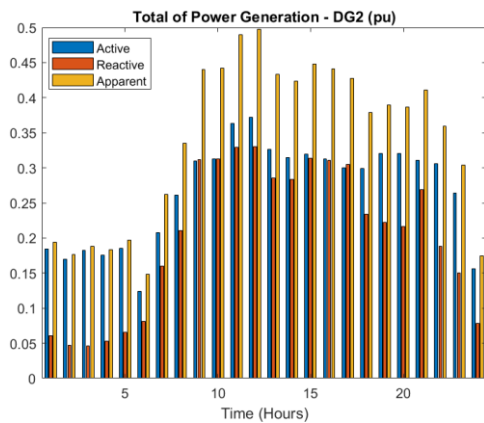
Figure 15. Power generation – DG1
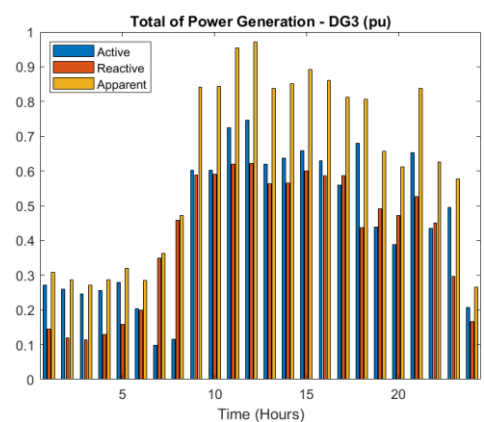

Figure 16. Power generation – DG2

Figure 17. Power generation – DG3

4. CONCLUSIONS

This paper presented an approach to defining the minimum amount of load to be shed, maintaining the steady-state frequency between pre-specified limits in islanded microgrids. An Optimal Power Flow has been proposed. The reference values of frequency and voltage of each DG unit, together with the droop coefficients, are considered as decision variables.

The approach was applied to a 33-bus islanded microgrid considering a planning horizon of 24 hours. Based on the obtained results, it was possible to see the effectiveness of the method, as the operation occurred meeting all the technical requirements.

However, important aspects associated with the problem's multimodal nature must be better investigated in the future to enhance the quality of the solutions (solutions near the global optima). The application of different optimization solvers, as well as metaheuristics, will be considered by the authors. Also, the impacts of energy storage systems will be addressed in future works.

ACKNOWLEDGMENT

REFERENCES

Alves, G. O., Pereira, J. L. R., La Gatta, P. O., Passos Filho, J. A., & Tomim, M. A. (2019). A new governor power flow formulation based on the current injections method. *International Journal of Electrical Power & Energy Systems*, *104*, 705–715. https://doi.org/10.1016/j.ijepes.2018.07.031

Bakar, N. N. A., Hassan, M. Y., Sulaima, M. F., Mohd Nasir, M. N., & Khamis, A. (2017). Microgrid and load shedding scheme during islanded mode: A review. *Renewable and Sustainable Energy Reviews*, *71*, 161–169. https://doi.org/10.1016/j.rser.2016.12.049

Baran, M. E., & Wu, F. F. (1989). Network reconfiguration in distribution systems for loss reduction and load balancing. *IEEE Transactions on Power Delivery*, *4*(2), 1401–1407. https://doi.org/10.1109/61.25627

de Nadai Nascimento, B., Zambroni de Souza, A. C., da Silva Neto, J. A., Sarmiento, J. E., & Alvez, C. A. (2021). Load-Margin Assessments in MicroGrids and the Influence of Power Electronic Converter Operation Mode. *Journal of Control, Automation and Electrical Systems*, *32*(1), 203–213. https://doi.org/10.1007/s40313-020-00651-3

Dommel, H., & Tinney, W. (1968). Optimal Power Flow Solutions. *IEEE Transactions on Power Apparatus and Systems*, *PAS-87*(10), 1866–1876. https://doi.org/10.1109/TPAS.1968.292150

Foroutan, V. B., Moradi, M. H., & Abedini, M. (2016). Optimal operation of autonomous microgrid including wind turbines. *Renewable Energy*, *99*, 315–324. https://doi.org/10.1016/j.renene.2016.07.008

Gómez-Expósito, A., Conejo, A. J., & Cañizares, C. (Eds.). (2017). *Electric Energy Systems*. CRC Press. https://doi.org/10.1201/9781420007275

Granville, S. (1994). Optimal reactive dispatch through interior point methods. *IEEE Transactions on Power Systems*, *9*(1), 136–146. https://doi.org/10.1109/59.317548

Gupta, Y., Doolla, S., Chatterjee, K., & Pal, B. C. (2021). Optimal DG Allocation and Volt–Var Dispatch for a Droop-Based Microgrid. *IEEE Transactions on Smart Grid*, *12*(1), 169–181. https://doi.org/10.1109/TSG.2020.3017952

Hemmatpour, M. H., Mohammadian, M., & Gharaveisi, A. A. (2016). Optimum islanded microgrid reconfiguration based on maximization of system loadability and minimization of power losses. *International Journal of Electrical Power & Energy Systems*, *78*, 343–355. https://doi.org/10.1016/j.ijepes.2015.11.040

Jithendranath, J., Das, D., & Guerrero, J. M. (2021). Probabilistic optimal power flow in islanded microgrids with load, wind and solar uncertainties including intermittent generation spatial correlation. *Energy*, *222*, 119847. https://doi.org/10.1016/j.energy.2021.119847

Kundur, P. (1994). *Power System Stability and Control*. McGraw-Hill .

La Gatta, P. O., Passos Filho, J. A., & Pereira, J. L. R. (2019). Tools for handling steady-state under-frequency regulation in isolated microgrids. *IET Renewable Power Generation*, *13*(4), 609–617. https://doi.org/10.1049/iet-rpg.2018.5172

Lopes, J. A. P., Moreira, C. L., & Madureira, A. G. (2006). Defining Control Strategies for MicroGrids Islanded Operation. *IEEE Transactions on Power Systems*, *21*(2), 916–924. https://doi.org/10.1109/TPWRS.2006.873018

Manna, D., Goswami, S. K., & Chattopadhyay, P. K. (2018). Optimisation of droop coefficients of multiple distributed generators in a micro-grid. *IET Generation, Transmission & Distribution*, *12*(18), 4108–4116. https://doi.org/10.1049/iet-gtd.2018.5548

MathWorks. (2020). *MATLAB Optimization Toolbox*.

Peres, W., Oliveira, E. J., Passos Filho, J. A., & Silva Junior, I. C. (2015). Coordinated tuning of power system stabilizers using bio-inspired algorithms. *International Journal of Electrical Power & Energy Systems*, *64*, 419–428. https://doi.org/10.1016/j.ijepes.2014.07.040

Pulendran, S., & Tate, J. (2017). Energy storage system control for prevention of transient under-frequency load shedding. *2017 IEEE Power & Energy Society General Meeting*, 1–1. https://doi.org/10.1109/PESGM.2017.8274452